Ultrasonics Sonochemistry 89 (2022) 106135

Contents lists available at ScienceDirect

Ultrasonics Sonochemistry

journal homepage: www.elsevier.com/locate/ultson

Effects of dual-frequency slit ultrasound on the enzymolysis of high-concentration hydrolyzed feather meal: Biological activities and structural characteristics of hydrolysates

Chen Hong [a], Jia-Qi Zhu [a], Yi-Ming Zhao [a,b], Haile Ma [a,b,*]

[a] School of Food and Biological Engineering, Jiangsu University, 301 Xuefu Road, Zhenjiang, Jiangsu 212013, China
[b] Institute of Food Physical Processing, Jiangsu University, 301 Xuefu Road, Jingkou District, Zhenjiang, Jiangsu 212013, China

ARTICLE INFO

Keywords:
Dual-frequency slit ultrasound (DFSU)
High-concentration feather meal
Ultrasound-assisted enzymolysis
Antioxidant activity
ACE inhibitory activity
Protein structure

ABSTRACT

Ultrasound-assisted enzymolysis has been applied to improve conventional enzymolysis, while there are rare reports on the application of ultrasound to high-concentration feather protein enzymolysis. Therefore, the feasibility of dual-frequency slit ultrasound (DFSU) for enzymolysis of high-concentration hydrolyzed feather meal (HFM), as well as the biological activities and structural characteristics of hydrolysates were investigated. The single-factor test was used to optimize the ultrasonic processing parameters: substrate concentration, frequency mode, intermittent ratio, power density, and time. The results showed that protein recovery rate and conversion rate increased by 6.08% and 18.63% under the optimal conditions (200 g/L, 28/80 kHz, 5:2 s/s, 600 W/L, and 3 h) compared with conventional enzymolysis, respectively. The macromolecular proteins in hydrolysates were converted into micromolecular peptides (< 500 Da) when treated by DFSU, and antioxidant activity and angiotensin-I-converting enzyme (ACE) inhibitory activity of hydrolysates were increased. Scanning electron microscopy (SEM) and atomic force microscopy (AFM) images illustrated the microstructure changes of feather protein particles in the ultrasound-assisted enzymatic hydrolysates of HFM (UEH), including more porous, smaller, and more uniform. Additionally, the conformation of protein molecules was significantly affected ($P < 0.05$), including the increase in free sulfhydryl (SH), the decrease in disulfide bond (SS) and surface hydrophobicity (H_0). Fourier transform infrared (FTIR) spectra analysis further showed that the secondary structure of feather proteins was modified with a reduction in α-helix, β-turn, and β-sheet, while an increase in random coil content was observed. These results indicated that DFSU could be a promising method to enhance high-concentration HFM for preparing peptide-rich hydrolysates with high antioxidant activity and ACE inhibitory activity.

1. Introduction

Hydrolyzed feather meal (HFM), which is also known as commercial feather meal, is the main product of feather waste after treated by hydrothermal processes. Due to easy availability and high protein content, it can be used as an alternative protein source in animal feed to lower costs [1,2]. Hydrothermal processes, as one of the most common methods for feather waste treatment, is to cook feathers at a high temperature and/or high pressure with the addition of acids or alkali. This process aims to destroy the structure of hard-to-degrade keratins in feathers and improve the solubility of feather components. Thus, keratins were converted into soluble proteins that can be digested and absorbed easily [3]. Nonetheless, hydrothermal treatment can cause excessive denaturation of certain amino acid sequences due to high

Abbreviations: DFSU, dual-frequency slit ultrasound; HFM, hydrolyzed feather meal; ACE, angiotensin-I-converting enzyme; SEM, scanning electron microscopy; AFM, atomic force microscopy; UEH, ultrasound-assisted enzymatic hydrolysates of HFM; SH, disulfide bond; SS, free sulfhydryl; H_0, surface hydrophobicity; FTIR, Fourier transform infrared; EFM, enzymatic feather meal; MW, molecular weight; PLC, programmable logic controller; DPPH, 1,1-diphenyl-2-picrylhydrazyl; ABTS, 2,2′-azino-bis-(3-ethylbenzothiazoline-6-sulfonic acid); $ABTS^+$, ABTS radical cation; PBS, phosphate-buffered saline; TCA, trichloroacetic acid; HEPES, 2-[4-(Hydroxyethyl)-1-piperazinyl]-ethane sulfonic acid; FAPGG, N-[3-(2-Furyl)acryloyl]-L-phenylalanyl-glycyl-glycine; SDS, sodium dodecyl sulfate; DNTB, 5,5′-dithiobis-(2-nitrobenzoic acid); ANS, 1-aniline-8-naphthalene sulfonic acid; CEH, conventional enzymatic hydrolysates of HFM.

* Corresponding author: School of Food and Biological Engineering, Jiangsu University, 301 Xuefu Road, Zhenjiang, Jiangsu 212013, China.
E-mail address: mhl@ujs.edu.cn (H. Ma).

https://doi.org/10.1016/j.ultsonch.2022.106135
Received 2 June 2022; Received in revised form 10 August 2022; Accepted 20 August 2022
Available online 24 August 2022

temperature or pressure, resulting in the loss of thermolabile amino acids and the formation of potentially toxic chemicals, such as lysinoalanine. These changes reduce the bioavailability and digestibility of HFM [4], as well as variable nutritional quality [5].

Due to the disadvantages of hydrothermal methods mentioned above, enzymolysis technology has been developed as an alternative technology, and enzymatic feather meal (EFM) is increasingly recognized as a viable source of dietary protein in food and feed supplements [6]. Feather proteins can be cleaved into micromolecular peptides after being hydrolyzed by enzymes, which are easy to digest and absorb for animals, and thus the biological potency is improved [7,8]. Poolsawat et al. [9] found that the coefficient digestibility of tilapia was increased after being fed with EFM that was hydrolyzed with protease (10 g/kg feather meal). In addition, keratin in feathers is rich in hydrophobic amino acid residues, accounting for 50–60% of the polypeptide chain. Enzymolysis is beneficial to increase the number of ionizable groups and the exposure of hydrophobic groups, which may also contribute to the bioactivity activities of protein hydrolysates and peptides [10]. Ohba et al. [11] reported that the antioxidant activity of enzymatic hydrolysates of chicken feathers was attributed to the large amounts of cysteine in keratin. Moreover, angiotensin-I-converting enzyme (ACE) inhibitory activity was increased with the decreasing molecular weight of hydrolysates. However, the cost of enzymolysis technology is too high, which is a big barrier to industrial adoption [12].

The combination of two or more methods has been proposed to compensate for the shortcomings of the single treatment described above. Thermo-enzymatic hydrolysis has been explored for the hydrolysis of keratin-rich materials. For example, Mokrejs et al. [13] demonstrated that keratin hydrolysates of chicken feathers could be obtained more efficiently under quite mild reaction conditions (8 h hydrolysis for 2% feathers at 70 °C with 5% enzyme dose). Similarly, Cheong et al. [14] also found that higher protein degradation and protein recovery were achieved via thermal-alkaline pretreatment combined with enzymatic treatment. It might be that thermal-alkaline pretreatment weakened the structure of chicken feathers, which enhanced the subsequent *Savinase* hydrolysis (4 h hydrolysis for 5% feathers). Although the combined technology can improve the enzymolysis of the feather meal, it is only applied to samples with low substrate concentrations at present. This disadvantage leads to a lower efficiency of enzymolysis and a higher cost for subsequent drying, which is opposite to the requirements of energy conservation and emission reduction. Therefore, developing a suitable high-concentration enzymolysis technology for low-solubility raw materials such as feathers has been of great importance for industrial applications.

As a green, efficient, safe, and novel physical processing technology, ultrasound has been widely used in assisting enzymolysis [15,16]. Acoustic cavitation generated by ultrasound technology causes mechanical effects as well as heat and chemical effects, which leads to the breakage of substrates and protein denaturation. These effects can improve the exposure of hydrophobic groups and the accessibility of the enzymes to the substrates [17]. Thereby, ultrasound can enhance the overall efficiency of the enzymolysis process, and even improve the yield and biological activities of enzymatic hydrolysates [18]. However, there are rare reports on the application of ultrasound to high-concentration enzymolysis. Hence, we investigated the feasibility of ultrasonic-assisted enzymolysis of high-concentration HFM using the peptide yield and protein conversion rate as the indices. The enzymolysis process parameters (substrate concentration, frequency mode, intermittent ratio, power density, and time) were optimized with the single-factor test. Under the optimal conditions, the protein recovery rate, molecular weight (MW) distribution, and bioactivities were evaluated, especially structure characterizations, which were studied by the examination of scanning electron microscopy (SEM), atomic force microscopy (AFM), free sulfhydryl (SH) and disulfide bond (SS) content, Fourier transform infrared (FTIR) spectra, and surface hydrophobicity (H_0).

2. Materials and methods

2.1. Materials

Raw hydrolyzed feather meal (HFM) (86.1% protein-Kjeldahl Method) made from chicken feathers was supplied by Qinhuangdao Yier Biological Technology Co., Ltd. (China). Alcalase (2.801×10^5 U/g) was obtained from Nanjing Chengna Chemical Co., Ltd. (China), which was selected from various proteases (i.e., Flavourzyme, Protamex, Papain, Neutrase, Trypsin, Alcalase, and Keratinase) for the enzymolysis in the preliminary experiments (data not shown). All reagents used in the experiment were of analytical grade.

2.2. Enzymolysis of HFM with dual-frequency slit ultrasound (DFSU) equipment

The ultrasound equipment (developed by Jiangsu University, Fig. 1a) is composed of the programmable logic controller (PLC), ultrasonic generators (20, 28, 40, 50, 68, and 80 kHz), and a slit cavity where ultrasonic transducers work. As shown in Fig. 1b, the HFM suspension (1 L) was pre-heated (50 °C, 20 min) utilizing a thermostatic bath, and circularly transported to the ultrasonic slit cavity using a peristaltic pump. Subsequently, the pH of the suspension was adjusted to 8.5 using 6 mol/L NaOH by an automatic potentiometric titration instrument, and the Alcalase with the amount of 10,000 U/g protein was added to initiate the reaction. The pH was maintained by the continuous addition of NaOH during the DFSU-assisted enzymolysis process. The initial ultrasound conditions were as follows: synchronous working of 20/68 kHz, ultrasonic intermittent ratio of 5:2 s/s, ultrasonic power density of 400 W/L, and ultrasonic time of 3 h. Additionally, ultrasonic parameters were optimized by the single-factor test, and the detailed parameters were shown in Table 1. The reaction was terminated by boiling the mixtures for 10 min. The hydrolysates were neutralized (pH 7.0) using 2 mol/L HCl after cooling to room temperature, and then centrifuged (15 min, 12,000 r/min) to obtain the supernatant for subsequent analysis. Conventional enzymolysis for 3 h without ultrasound treatment served as the control.

2.3. Determination of peptide yield and protein conversion rate

The peptide yield was defined as the mass of chicken feather peptides in enzymatic hydrolysates of HFM in 1 L reaction solution, which was calculated as follows:

$$Peptide\ yield\ \ (g) = \frac{C \times V}{1000} \tag{1}$$

where C is the concentration of peptides in hydrolysates (mg/mL), which was determined by the Folin-phenol method [19]; V is the volume of hydrolysates (mL).

The protein conversion rate represented the mass of chicken feather peptides prepared by 100 g of chicken protein, which was calculated via Eq. (2) [20]:

$$Protein\ \ \text{conversion rate}\ \ (\%) = \frac{C \times V}{10M} \tag{2}$$

where M is the mass of substrate protein (g).

In addition, the overall effect of HFM enzymolysis (A) was comprehensively evaluated by the peptide yield and protein conversion rate, and the evaluation formula was as follows:

$$A = 0.6 \times Protein\ conversion\ \ \text{rate} + 0.4 \times Peptide\ yield \tag{3}$$

2.4. Determination of soluble protein yield and protein recovery rate

Soluble protein yield was defined as the mass of soluble proteins in enzymatic hydrolysates of HFM in 1 L reaction solution, which was

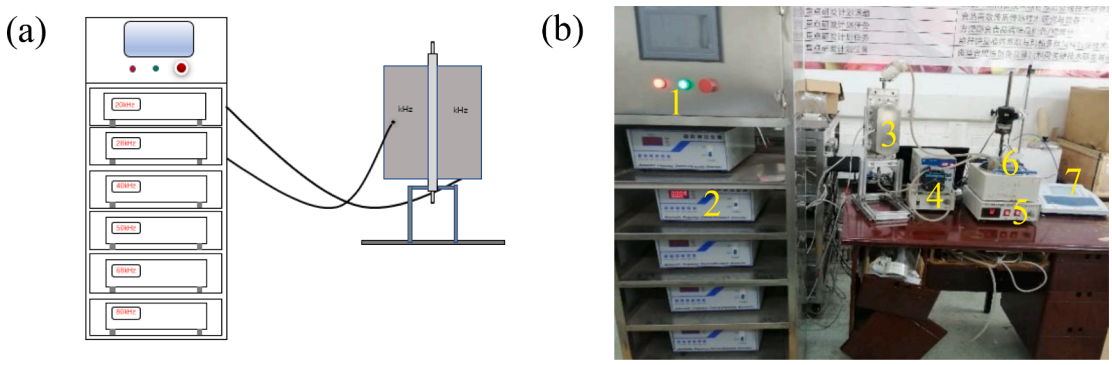

Fig. 1. The self-design DFSU-assisted enzymolysis system; (a): A schematic diagram of DFSU; (b): A photo of the whole enzymolysis system (1. Programmable Logic Controller (PLC) control panel; 2. Ultrasonic generator; 3. Slit cavity; 4. Peristaltic pump; 5. Thermostatic bath; 6. Reactor; 7. Automatic potentiometric titrator).

Table 1
Design of single-factor test parameters for ultrasound-assisted enzymolysis of HFM.

Factors	Levels
Substrate concentration	5%, 10%, 15%, 20%, and 25%
Ultrasonic frequency mode	single frequency: 20, 28, 40, 50, 68, and 80 kHz dual frequency: 20/28, 20/40, 20/50, 20/68, 20/80, 28/40, 28/40, 28/50, 28/68, 28/80, 40/50, 40/68, 40/80, 50/68, 50/80, and 68/80 kHz
Ultrasonic intermittent ratio	5:0, 5:1, 5:2, 5:3, and 5:4 s/s
Ultrasonic power density	300, 400, 500, 600, 700, and 800 W/L
Ultrasonic time	0.5, 1.0, 1.5, 2.0, 2.5, 3.0, and 3.5 h

computed in accordance with Eq. (4):

$$Soluble\ protein\ yield\ (g) = \frac{C_S \times V}{1000} \quad (4)$$

where *Cs* is the soluble protein content concentration (mg/mL), which was determined by the method of Wang et al. [21]; *V* is the volume of hydrolysates (mL).

The protein recovery rate represented the mass of soluble proteins obtained from 100 g of HFM, which was calculated according to the following equation [14]:

$$Protein\ recovery\ rate\ (\%) = \frac{C_S \times V}{10M_0} \quad (5)$$

where M_0 is the initial mass of HFM (g).

2.5. Determination of the antioxidant activity of enzymatic hydrolysates

2.5.1. 1,1-Diphenyl-2-picrylhydrazyl (DPPH) radical-scavenging activity assay

The radical-scavenging activity of enzymatic hydrolysates was measured by the method of Alahyaribeik et al. [22] with some modifications. The supernatant of enzymatic hydrolysates was freeze-dried in a freeze-dryer (Model 77530-30, Labconco Co., USA). Sample solutions with various concentrations were prepared by dissolving the freeze-dried hydrolysates in distilled water. Subsequently, 2 mL of sample solution (1.0, 2.0, 3.0, 4.0, and 5.0 mg/mL) was added to 2 mL of ethanol with 0.1 mmol/L DPPH, and then the mixtures were incubated for 30 min in the dark at room temperature. Absorbance was measured at 517 nm by the spectrophotometer (Unic 7200, Unocal Corporation, Shanghai, China). The DPPH radical scavenging activity was determined using the following equation:

$$DPPH\ radical\text{-}scavenging\ activity\ (\%) = (1\text{-}\frac{Ab_s}{Ab_c}) \times 100 \quad (6)$$

where Ab_s is the absorbance of the sample; Ab_c is the absorbance of distilled water. Further, the effective concentration (IC_{50}) that scavenged 50% of the free radicals was evaluated by using the radical-scavenging activity as a function of the protein concentration plot.

2.5.2. 2,2′-Azino-bis-(3-ethylbenzothiazoline-6-sulfonic acid) (ABTS) radical-scavenging activity assay

The method of Bezus et al. [23] was modified to determine ABTS radical-scavenging activity. The ABTS radical cation ($ABTS^+$) was produced by mixing 10 mL of 7 mmol/L ABTS with 10 mL of 5 mmol/L $K_2S_2O_8$ and allowing the mixture to rest in the dark for 12 h before use. The $ABTS^+$ solution was diluted with 0.1 mol/L phosphate-buffered saline (PBS, pH 7.4) to an absorbance of 0.7 ± 0.02 at 734 nm. Then 50 μL of the sample solution (0.1, 0.2, 0.3, 0.4, 0.5, and 0.6 mg/mL) was mixed with 250 μL of diluted $ABTS^+$ solution, and the mixture was measured at 734 nm by the spectrophotometer after 6 min. ABTS radical-scavenging activity was estimated using the following equation:

$$ABTS\ radical\text{-}scavenging\ activity\ (\%) = \frac{Ab_c\text{-}Ab_s}{Ab_c} \times 100 \quad (7)$$

where Ab_c is the absorbance of the control, which is distilled water here; Ab_s is the absorbance of the sample.

2.5.3. Reducing power assay

The reducing power of the sample was assessed using the method described by Bezus et al. [23] with some modifications. An admixture of 1 mL of the sample solution at different concentrations (2.0–10.0 mg/mL), 2.5 mL of PBS (0.2 mmol/L, pH 6.6) and 1 mL of 1% $K_3Fe(CN)_6 \cdot 3H_2O$ was incubated at 50 °C for 20 min. Then 12.5 mL of 10% trichloroacetic acid (TCA) was added, and the admixture was centrifuged at 5000 rpm for 10 min. Subsequently, 2.5 mL of the supernatant was taken and mixed with 0.5 mL of 0.1% $FeCl_3$ and 2.5 mL of distilled water. After incubation for 10 min, the absorbance of the mixture was measured at 700 nm by the spectrophotometer.

2.6. Determination of angiotensin-I-converting enzyme (ACE) inhibition rate of enzymatic hydrolysates

The ACE inhibitory activity of enzymatic hydrolysates was determined according to the method of Cui et al. [24]. 2-[4-(Hydroxyethyl)-1-piperazinyl]-ethane sulfonic acid (HEPES) buffer solution was prepared by dissolving 1.910 g of HEPES and 1.755 g of NaCl in an appropriate amount of distilled water. Then it was transferred into a 100-mL volumetric flask, and the distilled water was added to the volume. The pH was adjusted to 8.3. After that, 19.97 mg of N-[3-(2-Furyl)acryloyl]-L-

phenylalanyl-glycyl-glycine (FAPGG) was dissolved in HEPES buffer solution, and the volume was added to 50 mL. The FAPGG solution was stored at 4 °C in the dark for later use. Besides, the order of sample addition in the determination of the ACE inhibition rate was shown in Table 2, and the formula for calculating the inhibition rate of ACE was as follows:

$$ACE\ inhibition\ rate\ \ (\%) = \frac{(C_1\text{-}C_2)\text{-}(S_1\text{-}S_2)}{C_1\text{-}C_2} \times 100 \quad (8)$$

where C_1 and S_1 represent the initial absorbance of the blank hole and sample hole measured at 340 nm, respectively; C_2 and S_2 represent the absorbance of the blank hole and sample hole after holding at 37 °C for 30 min. All the data was obtained using the automatic microplate reader (Infinite 200 PRO, Tecan Trading AG, Switzerland). Further, the effective concentration (IC_{50}) that inhibited 50% of ACE activity was evaluated by using the ACE inhibition rate as a function of the protein concentration plot.

2.7. Molecular weight (MW) distribution of enzymatic hydrolysates

The MW distribution was determined with a high-performance gel filtration chromatography (Ultimate 3000; Thermo Scientific Inc., Waltham, MA, USA) [25]. The injection volume was kept at 10 μL at the flow rate of 0.5 mL/min and monitored at the wavelength of 220 nm. The standard calibration curve was plotted with cytochrome *C* (12400 Da), bacitracin (1450 Da), glycine-glycine-tyrosine-arginine (451 Da), and glycine-glycine-glycine (189 Da). Finally, Breeze software (Waters, MA, USA) was used to analyze the data.

2.8. Scanning electron microscopy (SEM)

The morphology of enzymatic hydrolysates was observed by SEM. The freeze-dried sample was placed on one surface of a two-sided adhesive tape, and it was coated with a thin gold layer. Then the sample was observed by a scanning electron microscope (Hitachi S-3400 N, Hitachi High Technologies, Tokyo, Japan) at the acceleration voltage of 15 kV.

2.9. Atomic force microscopy (AFM)

The freeze-dried sample was dissolved in 0.01 mol/L PBS (pH 7.8) to prepare a 1 mg/mL solution. Then 20 μL solution was dropped on a polished silicon wafer and dried for observation with MFP-3D AFM (Asylum Res. Inc., USA). The images obtained were analyzed by the Bruker offline software (Nanoscope Analysis 1.5, Bruker Inc., Karlsruhe, Germany).

2.10. Determination of the contents of free sulfhydryl (SH) and disulfide bond (SS)

The SH content was measured by Ellman's reagent method [26]. 10 mg/mL sample solution was prepared by Tris-Gly buffer (86 mmol/L Tris, 90 mmol/L Gly, and pH 8.0). Then 1 mL of sample solution was mixed with 5 mL of 0.5% sodium dodecyl sulfate (SDS), and 0.05 mL of Ellman's reagent solution [4 mg/mL 5,5′-dithiobis-(2-nitrobenzoic acid) (DTNB) in standard buffer] was added. After mixture, the solution was incubated for 30 min at 30 °C, and the absorbance at 412 nm was read by the spectrophotometer. The SH content (C_{SH}) was calculated by using the following formulas:

$$\Delta Abs_{412} = Abs_{with\ \ DNTB} - Abs_{without\ \ DNTB} \quad (9)$$

$$C_{SH}\ (\mu mol/g) = (73.53 \times \Delta Abs_{412} \times D)/C \quad (10)$$

where ΔAbs_{412} is the net absorbance measured at 412 nm; D is the dilution factor; C is the protein concentration (mg/mL).

The SS content was determined according to the method of Beveridge et al. [27] with some modifications. The admixture of 0.5 mL of the sample solution, 5 mL of Tris-Gly buffer plus 8 mol/L urea, and 0.1 mL of β-mercaptoethanol were incubated for 1 h at 25 °C, followed by the use of 12% TCA three times. The precipitate was collected and dissolved at 15 mL of 0.5% SDS, and 0.15 mL of Ellman's reagent was added for color development (30 °C, 30 min). The absorbance was also monitored at 412 nm to calculate the total SH content by Eq. (10). The SS content (C_{SS}) was assessed as follows:

$$C_{SS}\ (\mu mol/g) = \frac{C'_{SH} - C_{SH}}{2} \quad (11)$$

where C'_{SH} is the total SH content (μmol/g); C_{SH} is the free SH content (μmol/g).

2.11. Fourier transform infrared (FTIR) spectra measurement

The determination method of FTIR was modified according to Xu et al. [28]. The sample was mixed with KBr (1:11), milled to 2–3 μm, and pressed into a 1–2 mm slice. The slice was measured with an FTIR spectrometer (Nicolet IS50, Thermo Electron Corporation, USA), and the spectra were recorded in the range of 400–4000 cm^{-1}. Omnic 8.0 software (Thermo Fisher Scientific Inc., Waltham, MA) was used to analyze the FTIR spectral data. The data deconvolution, peak-separation, and fitting analysis of the amide I-band (1600–1700 cm^{-1}) were determined by PeakFit Version 4.12 software (SPSS Inc., Chicago, IL, USA).

2.12. Determination of surface hydrophobicity (H_0)

The hydrophobic index H_0 was determined by a fluorescence spectrophotometer using 1-aniline-8-naphthalene sulfonic acid (ANS) as a fluorescence probe [29]. Sample solution (1.0 mg/mL) was prepared by dissolving the freeze-dried hydrolysate in 0.01 mol/L phosphate buffer solution (PBS, pH 8.0), and then diluted with PBS to get a series of gradient protein concentrations (0.1, 0.2, 0.3, 0.4, and 0.5 mg/mL). Diluted solution (4 mL) was labeled with 20 μL of 8.0 mmol/L ANS solution (dissolved in 0.01 mol/L PBS, pH 8.0) in the dark for 10 min at room temperature, and the fluorescence intensity was measured by a fluorescent photometer (Varian Inc., Palo Alto, USA) at the excitation wavelength 380 nm and emission wavelength 400–550 nm (slit 5.0 nm). The scanning speed was 120 nm/min. The hydrophobic index H_0 was defined as the initial slope of the fluorescence intensity versus the protein concentration of the serial dilutions.

2.13. Statistical analysis

Analysis of variance (ANOVA) was performed and means were separated at the significance level of $P < 0.05$. All analyses including calculations were conducted with the aid of the statistical software Microsoft Excel 2016 and Origin 2018. Each determination was carried out in triplicate.

Table 2
Determination of ACE inhibition rate.

Component	The blank hole (μL)	The sample hole (μL)
ACE	50	50
HEPES buffer solution	100	0
Enzymatic hydrolysates	0	100
FAPGG	60	60

Note: ACE: angiotensin-I-converting enzyme; HEPES: 2-[4-(Hydroxyethyl)-1-piperazinyl]-ethane sulfonic acid; FAPGG: N-[3-(2-Furyl)acryloyl]-L-phenylalanyl-glycyl-glycine.

3. Results and discussion

3.1. Feasibility analysis of DFSU-assisted high-concentration enzymolysis

The effects of different substrate concentrations on the protein conversion rate, peptide yield, and A-value of enzymatic hydrolysates are illustrated in Fig. 2. Results showed that dual-frequency slit ultrasound (DFSU) could improve enzymolysis of hydrolyzed feather meal (HFM) regardless of low or high substance concentration, as well as protein conversion rate and peptide yield. Compared with the control, the overall enzymolysis effect (A-value) of HFM treated by DFSU was improved by 3.85%, 8.55%, 11.39%, 14.91%, and 10.01% with the substrate concentrations of 50, 100, 150, 200, and 250 g/L, respectively. The A-value reached the maximum of 76.68 at 200 g/L, where the protein conversion rate rose to 59.50%, and the yield of the peptides was 102.45 g. Additionally, a higher protein conversion rate was observed at the lower concentration of HFM (50 g/L) than at the high concentration. It might be that enzymes can fully bind to the substrates when the concentration is low. Nevertheless, the low concentration limited the peptide yield. Although more peptides were produced at the excessive concentration (250 g/L), the protein conversion rate was lower than that at 200 g/L, which may be because that excessive concentration increases the viscosity coefficient of the reaction system, causing an increase in the cavitation threshold and ultimately reducing cavitation bubbles [26]. The loss of acoustic waves is increased in the process of mass transfer and diffusion, which has a negative effect on enzymolysis and leads to a low protein conversion rate. In general, the technology of ultrasound-assisted enzymolysis of high-concentration HFM is feasible. The optimized HFM concentration was selected as 200 g/L for the following experiments, which is also more in accordance with industrial production requirements.

3.2. Effects of different ultrasonic working parameters on the enzymolysis of HFM

3.2.1. Effects of ultrasonic frequency mode on the enzymolysis of HFM

The effects of single-frequency treatment and dual-frequency treatment on enzymolysis are displayed in Fig. 3a and 3b, respectively. The results showed that the protein conversion rate, peptide yield, and A-value of ultrasound-assisted enzymatic hydrolysates of HFM (UEH) could be significantly increased under single-frequency treatment or dual-frequency treatment compared with conventional enzymatic hydrolysates of HFM (CEH) ($P < 0.05$). As shown in Fig. 3a, the protein conversion rate, peptide yield, and A-value improved gradually with the increase of frequency under the single-frequency ultrasound mode. They reached the maximum value at 80 kHz (58.29%, 100.37 g, and 75.12, respectively), where A-value increased by 12.58% compared with the control. Meanwhile, the protein conversion rate and peptide yield of UEH were the highest when the frequency was 28/80 kHz under the synchronous dual-frequency ultrasound mode, reaching 61.12% and 105.25 g, respectively (Fig. 3b). Moreover, the A-value of UEH was 18.05% higher than CEH at 28/80 kHz. Ultrasound is characterized as low frequency and high energy, and many studies have proved that ultrasonic frequency has a remarkably favorable influence on the enzymolysis of proteins [19,21,24]. Dual-frequency ultrasound had a better effect on enhancing enzymolysis of HFM than single-frequency ultrasound based on the above results. It might be because dual-flat has uniform energy dissipation over a wider area than single-flat ultrasound [30]. In addition, compared with the single frequency, the interaction between specific frequencies may produce dual-frequency synergies and the formation of new microbubble clusters with different characteristics, which can improve the efficiency of the whole process [31,32]. Therefore, the synchronous dual-frequency ultrasound 28/80 kHz was picked for subsequent experiments.

3.2.2. Effects of ultrasonic intermittent ratio on the enzymolysis of HFM

The ultrasonic intermittent ratio refers to the ratio of pulse operating time to pulse intermittent time. As can be seen from Fig. 3c, protein conversion rate, peptide yield, and A-value of UEH increased initially and then decreased with the increase in the ultrasonic intermittent ratio. The maximum protein conversion rate (61.12%), peptide yield (105.25 g), and A-value (78.77) were obtained when the ultrasonic intermittent ratio was 5:2 s/s. Similar trends were also reported by Wang et al. [26], where relative enzymolysis efficiency and protein dissolution rate of corn gluten meal also increased initially and then decreased with the increase of ultrasonic intermittent ratio. The initial increase may be related to the production of more cavitation bubbles at this ratio. While an excessive ultrasonic intermittent ratio may cause the collapse of

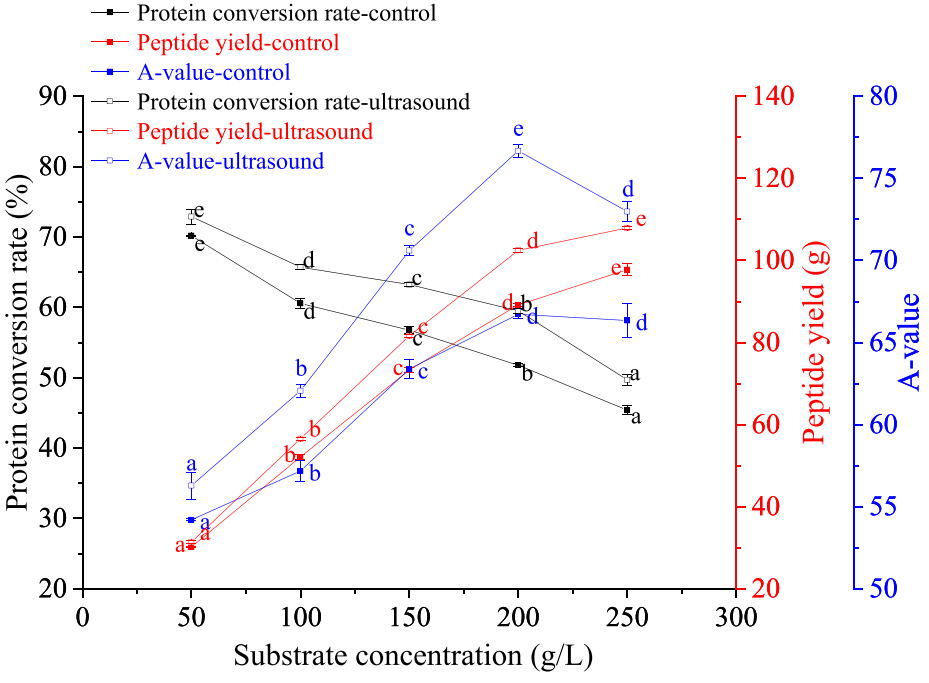

Fig. 2. Effects of different substrate concentrations on the protein conversion rate, peptide yield, and A-value of HFM under the conditions of ultrasound compared with the control. Control: conventional enzymolysis for 3 h; Ultrasound: ultrasound-assisted enzymolysis (frequency mode of 20/68 kHz, intermittent ratio of 5:2 s/s, power density of 400 W/L, and time of 3 h). The results are expressed as mean ± SD (n = 3). Different lowercase letters mean that the effects of different treatments are significantly different ($P < 0.05$).

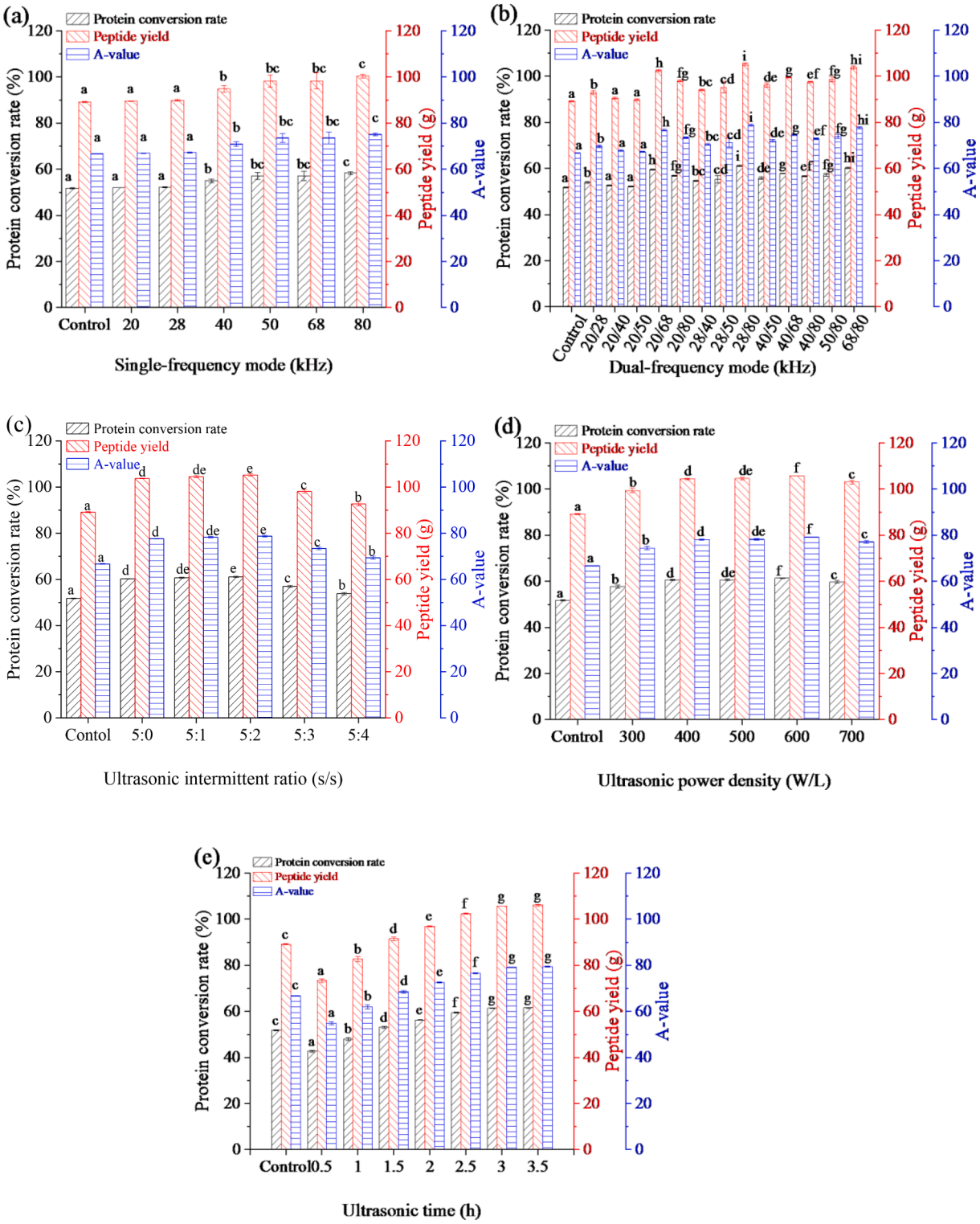

Fig. 3. Effects of different ultrasonic working parameters on protein conversion rate, peptide yield, and A-value of HFM compared with the control. Control: conventional enzymolysis for 3 h. (a) Single-frequency mode: substrate concentration of 200 g/L, intermittent ratio of 5:2 s/s, power density of 400 W/L, and time of 3 h; (b) Dual-frequency mode: substrate concentration of 200 g/L, intermittent ratio of 5:2 s/s, power density of 400 W/L, and time of 3 h; (c) Ultrasonic intermittent ratio: substrate concentration of 200 g/L, frequency mode of 28/80 kHz, power density of 400 W/L, and time of 3 h; (d) Ultrasonic power density: substrate concentration of 200 g/L, frequency mode of 28/80 kHz, intermittent ratio of 5:2 s/s, and time of 3 h; (e) Ultrasonic time: substrate concentration of 200 g/L, frequency mode of 28/80 kHz, intermittent ratio of 5:2 s/s, and power density of 600 W/L. The results are expressed as mean ± SD (n = 3). Different lowercase letters mean that the effects of different treatments are significantly different ($P < 0.05$).

bubbles before they are fully formed, leading to a decrease in cavitation intensity, which has a negative effect on enzymolysis. Therefore, the ultrasonic intermittent ratio of 5:2 s/s was selected.

3.2.3. Effects of ultrasonic power density on the enzymolysis of HFM

The effects of ultrasonic power density on the enzymolysis of HFM are shown in Fig. 3d. The protein conversion rate, peptide yield, and A-value increased firstly and then decreased as the power density increased, and the values reached the maximum of 61.42%, 105.76 g, and 79.16, respectively, when the ultrasonic power density was 600 W/L. Similar results were also found in the study of Wang et al. [26] and Wang et al [33], both of whom reported increased protein yield followed by decreased trend with increasing ultrasonic power. This increase is because ultrasonic cavitation effects increase with the improvement of ultrasonic power density [34]. The fragmentation of protein particles and the change of protein polymer conformation are aroused by improving cavitation effects, increasing the accessibility of enzymes to substrates. Nevertheless, excessive power density that surpasses the optimal value has a negative effect on enzymolysis. On the one hand, high-power density can produce excessive cavitation bubbles, resulting in a sound barrier [26]. On the other hand, high-power treatment leads to more exposure of non-polar groups, which enhances hydrophobicity between protein molecules. The increase of hydrophobicity, in turn, makes the exposed hydrophobic groups re-encased in protein, causing protein aggregation. Hence, it is not conducive to enzymolysis [35,36]. Therefore, the optimal ultrasonic power density was selected as 600 W/L based on the experimental results.

3.2.4. Effects of ultrasonic time on the enzymolysis of HFM

The effects of ultrasonic time on the enzymolysis of HFM are shown in Fig. 3e. As can be seen from the figure, the protein conversion rate, peptide yield, and A-value of UEH at 1.5 h was higher than that of CEH at 3 h, which indicated that DFSU improved the enzymolysis efficiency of HFM. The protein conversion rate, peptide yield, and A-value also increased as ultrasonic time increased, and the values reached the maximum (61.42%, 105.76 g, and 79.16, respectively) at 3 h. This phenomenon is because appropriate ultrasound time can refine and homogenize protein particles, increasing enzyme-substrate interactions remarkably [34,37]. However, prolonged ultrasonic treatment can cause excessive exposure of hydrophobic groups of protein, leading to protein aggregation and folding, which is harmful to enzymolysis [37,38]. Therefore, the optimal ultrasonic time was selected as 3 h.

3.3. Analysis of soluble protein yield and protein recovery rate

Protein is an important indicator for feather powder with a protein content of 80–91% [14]. As presented in Table 3, both the soluble protein yield and protein recovery rate of UEH were increased by 6.08% compared with CEH. The results were in agreement with the findings of Li et al. [39] and Wang et al. [26], in which ultrasonic-assisted enzymolysis can improve the protein dissolution rate.

Table 3
Determination of soluble protein yield and protein recovery rate of HFM.

Treatment	Soluble protein yield (g)	Protein recovery rate (%)
Control	127.59 ± 0.59^{a}	74.09 ± 0.34^{a}
Ultrasound	135.35 ± 0.12^{b}	78.60 ± 0.07^{b}

Note: Control: conventional enzymolysis for 3 h; Ultrasound: ultrasound-assisted enzymolysis (substrate concentration of 200 g/L, frequency mode of 28/80 kHz, intermittent ratio of 5:2 s/s, power density of 600 W/L, and time of 3 h); Values are means ± SD (three replicates); Different letters were used to show significant differences ($P < 0.05$) in the same column.

3.4. Determination of the antioxidative and antihypertensive potentials

Keratin has been considered as a source of bioactive peptides, and its hydrolysates have been proved to have the activity of antioxidant, antihypertension, and anti-diabetes [10,40]. In this study, three different supplementary methods were used to evaluate the antioxidant activity of enzymatic hydrolysates. As shown in Fig. 4, a higher 1,1-diphenyl-2-picrylhydrazyl (DPPH) scavenging activity, 2,2′-azino-bis-(3-ethylbenzothiazoline-6-sulfonic acid) (ABTS) scavenging activity, and reducing power of UEH were observed compared with CEH at the same concentration. The IC_{50} values of DPPH and ABTS scavenging activity of UEH were 3.41 mg/mL and 0.12 mg/mL, which were 17.25% and 21.96% lower than that of CEH, respectively. In general, ultrasound-assisted enzymolysis can improve the antioxidant activity of enzymatic hydrolysates. Many related studies have been reported [41–44]. For example, Wen et al. [42] showed that the antioxidant activity of arrowhead hydrolysates was improved by slit divergent ultrasound. Habinshuti et al. [44] also found that the antioxidation of sweet potatoes was increased via ultrasonic-assisted enzymolysis. Additionally, the IC_{50} values of DPPH and ABTS scavenging activity of UEH were also lower than that of feather hydrolysates obtained by feather-degrading *Bacillus* strains (DPPH IC_{50}: 15.12 mg/mL; ABTS IC_{50}: 5.39 mg/mL) and *Antarctic keratinolytic* bacterium (ABTS IC_{50}: 0.57 mg/mL) [23,45]. Moreover, the reducing power of UEH (0.13 Abs700 units in the presence of 2 mg/mL) was similar to that of feather hydrolysates reported by Callegaro et al. [45] (0.14 Abs700 units at 2.05 mg/mL), but lower than that of Bezus et al. [23] reported (2.19 Abs700 units at 2.03 mg/mL). These results showed that the feather hydrolysates obtained by ultrasound-assisted enzymolysis could show higher antioxidative activity than that produced by microbial conversion.

The anti-hypertensive activity of enzymatic hydrolysates was evaluated by the capability of hydrolysates to inhibit ACE activity. The ACE inhibition rate of enzymatic hydrolysates is displayed in Fig. 4d. The results showed that the ACE inhibition rate could be increased by ultrasonic-assisted enzymolysis technology. The IC_{50} value of UEH was 1.49 mg/mL, lower than that of CEH (1.91 mg/mL) and feather hydrolysates obtained by feather-degrading *Bacillus* strains (1.61 mg/mL) [44]. Similar results were observed by Ding et al. [46] and Ma et al. [30], who found that ultrasound decreased the IC_{50} value of grape seed hydrolysates and garlic powder hydrolysates. The increase in the antioxidant activity and ACE inhibition rate may be because ultrasound can change the structure of proteins, which leads to more release of active peptides during enzymolysis [40].

3.5. Effects of DFSU on the molecular weight (MW) distribution of enzymatic hydrolysates

The MW distribution of peptides is an important index to evaluate the quality of hydrolysates, and it is highly correlated to the activity of hydrolysates [21]. The MW distributions of UEH and CEH are presented in Table 4. The results showed that the MW distribution of UEH changed markedly compared with the control group. The fractions with MW > 3000 Da decreased, while the ones with MW < 500 Da increased. This phenomenon indicated that ultrasound-assisted enzymolysis could effectively convert macromolecular proteins into smaller molecular peptides and even free amino acids, which was in accordance with the result of Wang et al. [21]. It might be that DFSU can cause the exposure of hydrophobic residues or groups of HFM, which increases the active sites of Alcalase with a preference for sites containing hydrophobic residues [25]. Therefore, the enzymolysis reaction was promoted.

3.6. Scanning electron microscopy (SEM) and atomic force microscopy (AFM) analysis of enzymatic hydrolysates

The SEM images of enzymatic hydrolysates are shown in Fig. 5a and b. Feather protein particles in UEH became porous compared with the

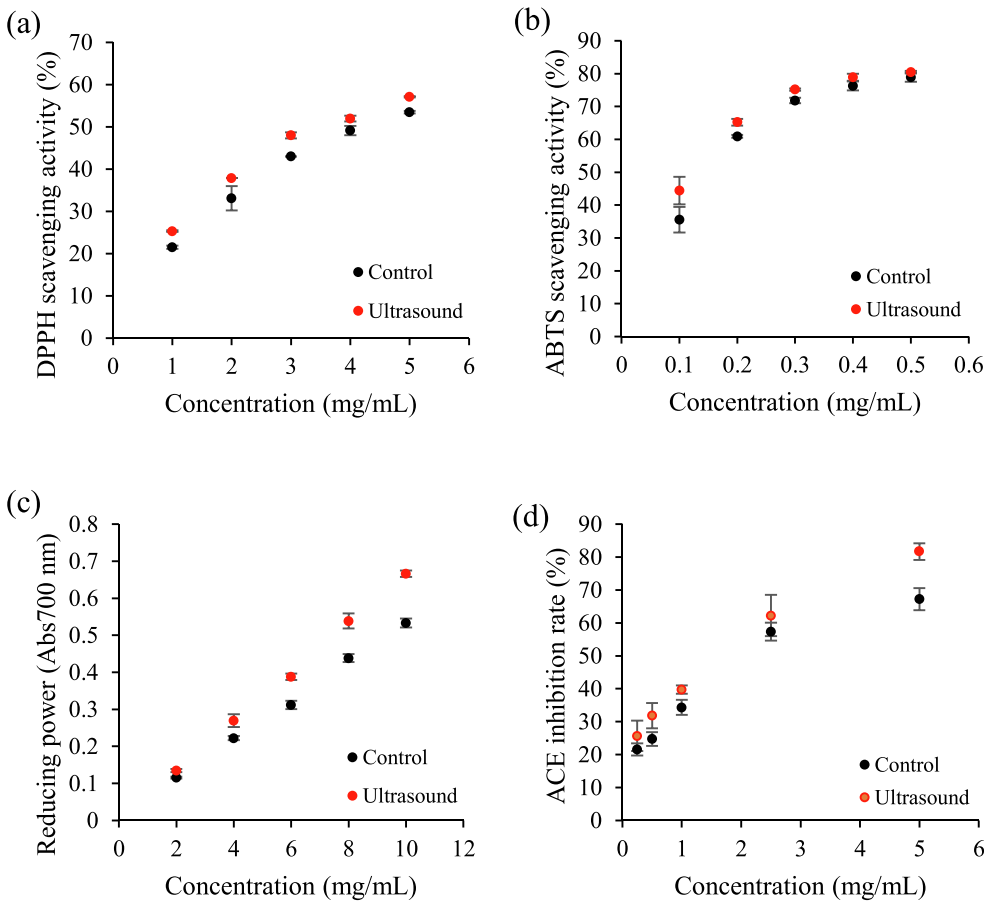

Fig. 4. Antioxidant and anti-hypertension potentials of ultrasound-assisted enzymatic hydrolysates compared with the control. (a) DPPH scavenging activity; (b) ABTS scavenging activity; (c) Reducing power; (d) ACE inhibition rate. Control: conventional enzymolysis for 3 h; Ultrasound: ultrasound-assisted enzymolysis (substrate concentration of 200 g/L, frequency mode of 28/80 kHz, intermittent ratio of 5:2 s/s, power density of 600 W/L, and time of 3 h). The results are expressed as mean ± SD (n = 3).

Table 4
Effects of ultrasound on the molecular weight distribution of enzymatic hydrolysates.

Molecular weight (Da)	Content	
	Control	Ultrasound
5000	15.00 ± 0.41^{b}	13.09 ± 0.58^{a}
3000–5000	7.92 ± 0.18^{b}	7.24 ± 0.35^{a}
1000–3000	18.70 ± 0.38^{a}	17.88 ± 0.50^{a}
500–1000	14.94 ± 0.76^{a}	15.31 ± 0.58^{a}
200–500	36.97 ± 0.45^{a}	38.83 ± 0.76^{b}
< 200	6.47 ± 0.44^{a}	7.65 ± 0.28^{b}

Note: Control: conventional enzymolysis for 3 h; Ultrasound: ultrasound-assisted enzymolysis (substrate concentration of 200 g/L, frequency mode of 28/80 kHz, intermittent ratio of 5:2 s/s, power density of 600 W/L, and time of 3 h); Values are means ± SD (three replicates); Different letters were used to show significant differences ($P < 0.05$) in the same row.

ones in CEH. This kind of structure can help the enzymes to enter into the protein molecules smoothly and cause more release of internal hydrophobic groups. More morphology details can be observed from topographic images by AFM analysis (as shown in Fig. 5c and 5d). It can be clearly seen from Fig. 5c that the topography of CEH presented a series of aggregation phenomena, while the diameter and height of the protein aggregates decreased considerably after ultrasound treatment (Fig. 5d), which made protein particles look smaller and evenly distributed in size. These results were in similitude to the findings of Xu et al. [28] and Wang et al. [26]. For example, Xu et al. [28] found that lots of little voids appeared in casein structure subjected to ultrasound treatment. Casein particles became smaller, and the number of protein particles increased sharply. These phenomena were conducive to the increase in the contact areas between enzymes and protein particles, facilitating the enzymolysis reaction.

3.7. Effects of DFSU on the contents of free sulfhydryl (SH) and disulfide bond (SS)

As an essential covalent bond to maintain the stability of protein spatial structure, the SS is closely related to the functional properties of proteins [43]. The changes in the contents of SH and SS represent the stretch and aggregation of proteins. Effects of ultrasound on the contents of SH and SS are displayed in Table 5. As can be seen from the table, ultrasound treatment significantly increased the content of SH and decreased the content of SS in feather proteins compared with the control group ($P < 0.05$). Results were consistent with the findings of Cui et al. [24]. It might be that the cavitation effects caused by ultrasound such as micro jets, shear forces, shock waves, and turbulence break SS in the proteins, causing the decomposition of SS and the formation of SH [20,47]. In addition, the protein molecules are stretched with the decomposition of SS, which causes more exposure of internal SH groups [26]. Moreover, the reduction of protein particle size after ultrasound treatment also increases the exposure of buried SH groups [20].

3.8. Effects of DFSU on the secondary structure

The relative contents of α-helix, β-sheet, β-turn, and random coil in proteins were observed by analyzing the C═O stretching vibration of the amide I-band (1600–1700 cm^{-1}) obtained from Fourier transform infrared (FTIR) spectra. As shown in Table 5, compared with CEH, the contents of α-helix, β-sheet, and β-turn of UEH decreased by 8.96%, 3.27%, and 4.55%, respectively, and the content of random coil increased by 28.13%. Results showed that ultrasound could transform

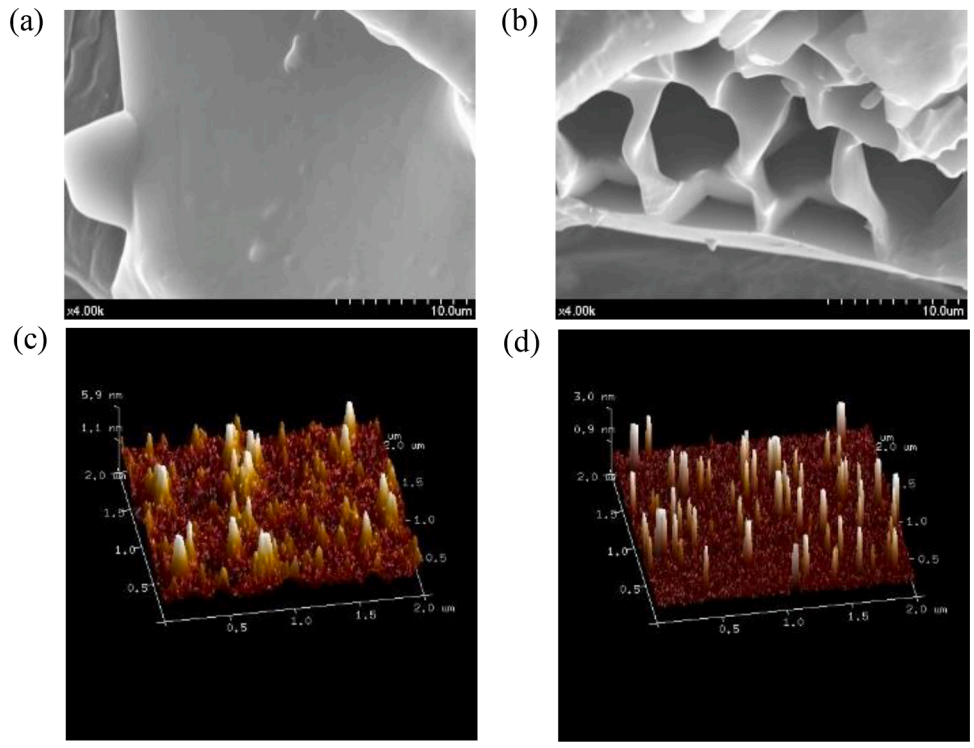

Fig. 5. The SEM and AFM analysis of enzymatic hydrolysates. (a) SEM image of CEH; (b) SEM image of UEH; (c) AFM image of CEH; (d) AFM image of UEH. SEM: scanning electron microscopy; AFM: atomic force microscopy; CEH: conventional enzymolysis hydrolysates of HFM; UEH: ultrasound-assisted enzymolysis hydrolysates of HFM.

Table 5
Effects of ultrasound pretreatment on the free sulfhydryl content (SH) content, disulfide bond (SS) content, surface hydrophobicity (H_0), and secondary structure.

Treatment	H_0	SS (μmol/g)	SH (μmol/g)	Secondary structure content (%)			
				α-helix	β-folding	β-corner	Random coil
Control	235.35 ± 3.08^a	1.91 ± 0.05^b	5.10 ± 0.10^a	14.80 ± 0.03^b	43.43 ± 0.23^b	27.55 ± 0.11^b	14.22 ± 0.05^a
Ultrasound	289.30 ± 2.25^b	0.19 ± 0.03^a	5.72 ± 0.08^b	13.47 ± 0.07^a	42.01 ± 0.13^a	26.30 ± 0.10^a	18.22 ± 0.11^b

Note: Control: conventional enzymolysis for 3 h; Ultrasound: ultrasound-assisted enzymolysis (substrate concentration of 200 g/L, frequency mode of 28/80 kHz, intermittent ratio of 5:2 s/s, power density of 600 W/L, and time of 3 h); Values are means ± SD (three replicates); Different letters were used to show significant differences ($P < 0.05$) in the same column.

the structure of α-helix, β-sheet, and β-turn into a random coil. Similar results were observed in the hydrolysates of casein, gluten, and milk protein after ultrasound treatment [24,28,48]. It might be that cavitation action weakens the hydrogen bonds that maintain the stability of protein, making the ordered structure converted into a disordered structure. These changes are more beneficial to the exposure of enzyme cleavage sites [21].

3.9. Effects of DFSU on the surface hydrophobicity (H_0) of enzymatic hydrolysates

The effects of DFSU on H_0 are shown in Table 5. The H_0 of UEH increased by 22.92% compared with CEH. These findings were consistent with the previous studies of corn proteins [20], milk proteins [24], rice proteins [29], and wheat germ proteins [49]. The increase in H_0 indicates that the interaction between hydrophobic linkages of the protein molecules is disrupted due to the ultrasound-induced cavitation effects, causing the exposure of hydrophobic groups that are buried in the interior protein. It has been reported that the hydrophobicity of protein is one of the important factors affecting ACE inhibitory activity and antioxidant activity of protein hydrolysates [29,50]. The increase in H_0 of UEH can improve the bioactivities of enzymatic hydrolysates.

4. Conclusions

As new ultrasound equipment, dual-frequency slit ultrasound (DFSU) provided an effective approach to realizing the high-concentration enzymolysis of low-dissolution materials such as feathers. The optimal DFSU treatment for hydrolyzed feather meal (HFM) enzymolysis (200 g/L, 28/80 kHz, intermittent ratio of 5:2 s/s, 600 W/L, and 3 h) was obtained from the single-factor test, under which the soluble protein yield and peptide yield increased by 6.08% and 18.63%, respectively, compared with the control. The antioxidant activity and angiotensin-I-converting enzyme (ACE) inhibitory activity of ultrasound-assisted enzymatic hydrolysates of HFM (UEH) were remarkably increased. It may be that the macromolecular proteins were converted into micromolecular peptides after DFSU treatment, which can be proved by the results of molecular weight (MW). The morphology of feather protein particles in the enzymatic hydrolysates observed by scanning electron microscopy (SEM) and atomic force microscopy (AFM) illustrated that the contact areas between enzymes and feather proteins were increased due to the formation of protein poriferous structure and the decrease in the protein particle sizes under DFSU-assisted enzymolysis. Moreover, the breakage of disulfide bond (SS), the alteration of secondary structure from ordered to disordered structure, and the increase of hydrophobic groups further indicated the change in the structure of feather protein

molecules. These conformational changes could be conducive to the combination of HFM and Alcalase and the improvement of antioxidant activity and ACE inhibitory activity of enzymatic hydrolysates. In conclusion, ultrasound can change the molecular conformation of feather protein particles in the enzymatic hydrolysates and enhance the conventional enzymolysis reaction, which provides the feasibility of high-concentration enzymolysis for feather meal with low solubility.

CRediT authorship contribution statement

Chen Hong: Conceptualization, Methodology, Data curation, Writing – original draft. **Jia-Qi Zhu:** Conceptualization, Methodology, Formal analysis, Data curation. **Yi-Ming Zhao:** Visualization, Formal analysis, Writing – review & editing. **Haile Ma:** Conceptualization, Funding acquisition, Supervision, Resources.

Declaration of Competing Interest

The authors declare that they have no known competing financial interests or personal relationships that could have appeared to influence the work reported in this paper.

Data availability

Data will be made available on request.

Acknowledgments

The authors gratefully acknowledge the support of the Primary Research & Development Plan of Jiangsu Province (BE2018368) and the Senior Talent Program of Jiangsu University (5501360012).

References

[1] P. Psofakis, I.T. Karapanagiotidis, E.E. Malandrakis, E. Golomazou, A. Exadactylos, E. Mente, Effect of fishmeal replacement by hydrolyzed feather meal on growth performance, proximate composition, digestive enzyme activity, haematological parameters and growth-related gene expression of gilthead seabream (*Sparus aurata*), Aquaculture 521 (2020), 735006, https://doi.org/10.1016/j.aquaculture.2020.735006.

[2] I. Campos, L. Valente, E. Matos, P. Marques, F. Freire, Life-cycle assessment of animal feed ingredients: poultry fat, poultry by-product meal and hydrolyzed feather meal, J. Cleaner Prod. 252 (2020), 119845, https://doi.org/10.1016/j.jclepro.2019.119845.

[3] G. Coward-Kelly, V.S. Chang, F.K. Agbogbo, M.T. Holtzapple, Lime treatment of keratinous materials for the generation of highly digestible animal feed: 1. Chicken feathers, Bioresour. Technol. 97 (2006) 1337–1343, https://doi.org/10.1016/j.biortech.2005.05.021.

[4] K. Callegaro, A. Brandelli, D.J. Daroit, Beyond plucking: feathers bioprocessing into valuable protein hydrolysates, Waste Manage. 95 (2019) 399–415, https://doi.org/10.1016/j.wasman.2019.06.040.

[5] K. Chojnacka, H. Gorecka, I. Michalak, H. Gorecki, A review: Valorization of keratinous materials, Waste Biomass Valoriz. 2 (2011) 317–321, https://doi.org/10.1007/s12649-011-9074-6.

[6] L. Pan, X.K. Ma, X.K.H.L. Wang, X. Xu, Z.K. Zeng, Q.Y. Tian, P.F. Zhao, S. Zhang, Z. Y. Yang, X.S. Piao, Enzymatic feather meal as an alternative animal protein source in diets for nursery pigs, Anim. Feed Sci. Technol. 212 (2016) 112–121, https://doi.org/10.1016/j.anifeedsci.2015.12.014.

[7] E. Tiwary, R. Gupta, Rapid conversion of chicken feather to feather meal using dimeric keratinase from *Bacillus licheniformis* ER-15, J. Bioprocess. Biotech. 2 (2012) 123, https://doi.org/10.4172/2155-9821.1000123.

[8] G.F.E. Pacheco, J.G. Pezzali, A. de Mello Kessler, L. Trevizan, Inclusion of exogenous enzymes to feathers during processing on the digestible energy content of feather meal for adult dogs, Revista Brasileira de Zootecnia. 45 (2016) 288–294, https://doi.org/10.1590/S1806-92902016000600002.

[9] L. Poolsawat, H. Yang, Y.-F. Sun, X.-Q. Li, G.-Y. Liang, X.-J. Leng, Effect of replacing fish meal with enzymatic feather meal on growth and feed utilization of tilapia (*Oreochromis niloticus* × *O. aureus*), Anim. Feed Sci. Technol. 274 (2021) 114895, https://doi.org/10.1016/j.anifeedsci.2021.114895.

[10] I. Sinkiewicz, H. Staroszczyk, A. Śliwińska, Solubilization of keratins and functional properties of their isolates and hydrolysates, J. Food Biochem. 42 (2018) 12494, https://doi.org/10.1111/jfbc.12494.

[11] R. Ohba, T. Deguchi, M. Kishikawa, F. Arsyad, S. Morimura, K. Kida, Physiological functions of enzymatic hydrolysates of collagen or keratin contained in livestock and fish waste, Food Sci. Technol. Res. 9 (2003) 91–93, https://doi.org/10.3136/fstr.9.91.

[12] Y. Hou, Z. Wu, Z. Dai, G. Wang, G. Wu, Protein hydrolysates in animal nutrition: industrial production, bioactive peptides, and functional significance, J. Anim. Sci. Biotechnol. 8 (2017) 24, https://doi.org/10.1186/s40104-017-0153-9.

[13] P. Mokrejs, P. Svoboda, J. Hrncirik, D. Janacova, V. Vasek, Processing poultry feathers into keratin hydrolysate through alkaline-enzymatic hydrolysis, Waste Manage. Res. 29 (2011) 260–267, https://doi.org/10.1177/0734242X10370378.

[14] C.W. Cheong, Y.S. Lee, S.A. Ahmad, P.T. Ooi, L.Y. Phang, Chicken feather valorization by thermal alkaline pretreatment followed by enzymatic hydrolysis for protein-rich hydrolysate production, Waste Manage. 79 (2018) 658–666, https://doi.org/10.1016/j.wasman.2018.08.029.

[15] C. Ozuna, I. Paniagua-Martínez, E. Castaño-Tostado, L. Ozimek, S.L. Amaya-Llano, Innovative applications of high-intensity ultrasound in the development of functional food ingredients: Production of protein hydrolysates and bioactive peptides, Food Res. Int. 77 (2015) 685–696, https://doi.org/10.1016/j.foodres.2015.10.015.

[16] B. Xu, S.M.R. Azam, M. Feng, B. Wu, W. Yan, C. Zhou, H. Ma, Application of multi-frequency power ultrasound in selected food processing using large-scale reactors: A review, Ultrason. Sonochem. 81 (2021), 105855, https://doi.org/10.1016/j.ultsonch.2021.105855.

[17] D. Wang, L. Yan, X. Ma, W. Wang, M. Zou, J. Zhong, T. Ding, X. Ye, D. Liu, Ultrasound promotes enzymatic reactions by acting on different targets: enzymes, substrates and enzymatic reaction systems, Int. J. Biol. Macromol. 119 (2018) 453–461, https://doi.org/10.1016/j.ijbiomac.2018.07.133.

[18] E.C. Umego, R. He, W. Ren, H. Xu, H. Ma, Ultrasonic-assisted enzymolysis: principle and applications, Process. Biochem. 100 (2020) 59–68, https://doi.org/10.1016/j.procbio.2020.09.033.

[19] X. Yang, Y. Li, S. Li, A.O. Oladejo, S. Ruan, Y. Wang, S. Huang, H. Ma, Effects of ultrasound pretreatment with different frequencies and working modes on the enzymolysis and the structure characterization of rice protein, Ultrason. Sonochem. 38 (2017) 19–28, https://doi.org/10.1016/j.ultsonch.2017.02.026.

[20] J. Jin, H. Ma, K. Wang, A.E.A. Yagoub, J. Owusu, W. Qu, R. He, C. Zhou, X. Ye, Effects of multi-frequency power ultrasound on the enzymolysis and structural characteristics of corn gluten meal, Ultrason. Sonochem. 24 (2015) 55–64, https://doi.org/10.1016/j.ultsonch.2014.12.013.

[21] Y. Wang, Z. Zhang, R. He, B.K. Mintah, M. Dabbour, W. Qu, D. Liu, H. Ma, Proteolysis efficiency and structural traits of corn gluten meal: Impact of different frequency modes of a low-power density ultrasound, Food Chem. 344 (2021), 128609, https://doi.org/10.1016/j.foodchem.2020.128609.

[22] S. Alahyaribeik, S.D. Sharifi, F. Tabandeh, S. Honarbakhsh, S. Ghazanfari, Stability and cytotoxicity of DPPH inhibitory peptides derived from biodegradation of chicken feather, Protein Expr. Purif. 177 (2021), 105748, https://doi.org/10.1016/j.pep.2020.105748.

[23] A. Bezus, F. Ruscasso, G. Garmendia, S. Vero, I. Cavello, S. Cavalitto, Revalorization of chicken feather waste into a high antioxidant activity feather protein hydrolysate using a novel psychrotolerant bacterium, Biocatal. Agric. Biotechnol. 32 (2021), 101925, https://doi.org/10.1016/j.bcab.2021.101925.

[24] P. Cui, X. Yang, Q. Liang, S. Huang, F. Lu, J. Owusu, X. Ren, H. Ma, Ultrasound-assisted preparation of ace inhibitory peptide from milk protein and establishment of its in-situ real-time infrared monitoring model, Ultrason. Sonochem. 62 (2020), 104859, https://doi.org/10.1016/j.ultsonch.2019.104859.

[25] J. Jin, H. Ma, B. Wang, E.G.A. Yagoub, K. Wang, R. He, C. Zhou, Effects and mechanism of dual-frequency power ultrasound on the molecular weight distribution of corn gluten meal hydrolysates, Ultrason. Sonochem. 30 (2016) 44–51, https://doi.org/10.1016/j.ultsonch.2015.11.021.

[26] Y. Wang, Z. Zhang, R. He, D. Liu, B.K. Mintah, M. Dabbour, H. Ma, Improvement in enzymolysis efficiency and changes in conformational attributes of corn gluten meal by dual-frequency slit ultrasonication action, Ultrason. Sonochem. 64 (2020), 105038, https://doi.org/10.1016/j.ultsonch.2020.105038.

[27] T. Beveridge, S.J. Toma, S. Nakai, Determination of SH-and SS-groups in some food proteins using Ellman's reagent, J. Food Sci. 39 (1974) 49–51, https://doi.org/10.1111/j.1365-2621.1974.tb00984.x.

[28] B. Xu, J. Yuan, L. Wang, F. Lu, B. Wei, R.S.M. Azam, X. Ren, C. Zhou, H. Ma, B. Bhandari, Effect of multi-frequency power ultrasound (MFPU) treatment on enzyme hydrolysis of casein, Ultrason. Sonochem. 63 (2020), 104930, https://doi.org/10.1016/j.ultsonch.2019.104930.

[29] Y. Ding, Y. Wang, W. Qu, X. Ren, F. Lu, W. Tian, J. Quaisie, S.M.R. Azam, H. Ma, Effect of innovative ultrasonic frequency excitation modes on rice protein: Enzymolysis and structure, LWT – Food Sci. Technol. 153 (2022), 112435, https://doi.org/10.1016/j.lwt.2021.112435.

[30] H. Ma, L. Huang, L. Peng, Z. Wang, Q. Rong, Pretreatment of garlic powder using sweep frequency ultrasound and single frequency countercurrent ultrasound: optimization and comparison for ACE inhibitory activities, Ultrason. Sonochem. 23 (2015) 109–115, https://doi.org/10.1016/j.ultsonch.2014.10.020.

[31] N.B. Waldo, C.D. Vecitis, Combined effects of phase-shift and power distribution on efficiency of dual-high-frequency sonochemistry, Ultrason. Sonochem. 41 (2018) 100–108, https://doi.org/10.1016/j.ultsonch.2017.09.010.

[32] T.J. Tiong, D.K.L. Liew, R.C. Gondipon, R.W. Wong, Y.L. Loo, M.S.T. Lok, S. Manickam, Identification of active sonochemical zones in a triple frequency ultrasonic reactor via physical and chemical characterization techniques, Ultrason. Sonochem. 35 (2017) 569–576, https://doi.org/10.1016/j.ultsonch.2016.04.029.

[33] Q. Wang, Y. Wang, M. Huan, K. Hayat, N.C. Kurtz, X. Wu, M. Ahmad, F. Zheng, Ultrasound-assisted alkaline proteinase extraction enhances the yield of pecan protein and modifies its functional properties, Ultrason. Sonochem. 80 (2021), 105789, https://doi.org/10.1016/j.ultsonch.2021.105789.

[34] Q. Li, X. Zhang, S. Tang, S. Mi, L. Lu, Q. Zeng, M. Xia, Z. Cai, Improved effect of ultrasound-assisted enzymolysis on egg yolk powder: Structural properties,

hydration properties and stability characteristics, Food Chem. 382 (2022), 132549, https://doi.org/10.1016/j.foodchem.2022.132549.
[35] C. Arzeni, K. Martínez, P. Zema, A. Arias, O.E. Pérez, A.M.R. Pilosof, Comparative study of high intensity ultrasound effects on food proteins functionality, J. Food Eng. 108 (2012) 463–472, https://doi.org/10.1016/j.jfoodeng.2011.08.018.
[36] L. Jiang, J. Wang, Y. Li, Z. Wang, J. Liang, R. Wang, Y. Chen, W. Ma, B. Qi, M. Zhang, Effects of ultrasound on the structure and physical properties of black bean protein isolates, Food Res. Int. 62 (2014) 595–601, https://doi.org/10.1016/j.foodres.2014.04.022.
[37] L. Lin, H. Cui, R. He, L. Liu, C. Zhou, W. Mamdouh, H. Ma, Effect of ultrasonic treatment on the morphology of casein particles, Ultrason. Sonochem. 21 (2014) 513–519, https://doi.org/10.1016/j.ultsonch.2013.08.017.
[38] P.B. Stathopulos, G.A. Scholz, Y.M. Hwang, J. Rumfeldt, J.R. Lepock, E. Meiering, Sonication of proteins causes formation of aggregates that resemble amyloid, Protein Sci. 13 (2004) 3017–3027, https://doi.org/10.1110/ps.04831804.
[39] S. Li, X. Yang, Y. Zhang, H. Ma, Q. Liang, W. Qu, R. He, C. Zhou, G.K. Mahunu, Effects of ultrasound and ultrasound assisted alkaline pretreatments on the enzymolysis and structural characteristics of rice protein, Ultrason. Sonochem. 31 (2016) 20–28, https://doi.org/10.1016/j.ultsonch.2015.11.019.
[40] V. Ferraro, M. Anton, V. Santé-Lhoutellier, The "sisters" α-helices of collagen, elastin and keratin recovered from animal by-products: functionality, bioactivity and trends of application, Trends Food Sci. Technol. 51 (2016) 65–75, https://doi.org/10.1016/j.tifs.2016.03.006.
[41] G.J. Fadimu, H. Gill, A. Farahnaky, T. Truong, Improving the enzymolysis efficiency of lupin protein by ultrasound pretreatment: Effect on antihypertensive, antidiabetic and antioxidant activities of the hydrolysates, Food Chem. 383 (2022), 132457, https://doi.org/10.1016/j.foodchem.2022.132457.
[42] F.F. Liu, Y.Q. Li, G.J. Sun, C.Y. Wang, Y. Liang, X.Z. Zhao, J.X. He, H.Z. Mo, Influence of ultrasound treatment on the physicochemical and antioxidant properties of mung bean protein hydrolysate, Ultrason. Sonochem. 84 (2022), 105964, https://doi.org/10.1016/j.ultsonch.2022.105964.
[43] C. Wen, J. Zhang, J. Zhou, Y. Duan, H. Zhang, H. Ma, Effects of slit divergent ultrasound and enzymatic treatment on the structure and antioxidant activity of arrowhead protein, Ultrason. Sonochem. 49 (2018) 294–302, https://doi.org/10.1016/j.ultsonch.2018.08.018.
[44] I. Habinshuti, T.H. Mu, M. Zhang, Structural, antioxidant, aroma, and sensory characteristics of maillard reaction products from sweet potato protein hydrolysates as influenced by different ultrasound-assisted enzymatic treatments, Food Chem. 36 (2021), 130090, https://doi.org/10.1016/j.foodchem.2021.130090.
[45] K. Callegaro, N. Welter, D.J. Daroit, Feathers as bioresource: Microbial conversion into bioactive protein hydrolysates, Process. Biochem. 75 (2018) 1–9, https://doi.org/10.1016/j.procbio.2018.09.002.
[46] Q. Ding, T. Zhang, S. Niu, F. Cao, R.A. Wu-Chen, L. Luo, H. Ma, Impact of ultrasound pretreatment on hydrolysate and digestion products of grape seed protein, Ultrason. Sonochem. 42 (2017) 704–713, https://doi.org/10.1016/j.ultsonch.2017.11.027.
[47] R. Zhao, X. Liu, W. Liu, Q. Liu, L. Zhang, H. Hu, Effect of high-intensity ultrasound on the structural, rheological, emulsifying and gelling properties of insoluble potato protein isolates, Ultrason. Sonochem. 85 (2022), 105969, https://doi.org/10.1016/j.ultsonch.2022.105969.
[48] C. Zhou, J. Hu, X. Yu, A.E.A. Yagoub, Y. Zhang, H. Ma, X. Gao, P.N.Y. Otu, Heat and/or ultrasound pretreatments motivated enzymolysis of corn gluten meal: Hydrolysis kinetics and protein structure, LWT – Food Sci. Technol. 77 (2017) 488–496, https://doi.org/10.1016/j.lwt.2016.06.048.
[49] J. Jia, H. Ma, W. Zhao, Z. Wang, W. Tian, L. Luo, R. He, The use of ultrasound for enzymatic preparation of ACE-inhibitory peptides from wheat germ protein, Food Chem. 119 (2010) 336–342, https://doi.org/10.1016/j.foodchem.2009.06.036.
[50] H.M. Chen, K. Muramoto, F. Yamauchi, Structural analysis of antioxidative peptides from soybean β-conglycinin, J. Agric. Food Chem. 43 (1995) 574–578, https://doi.org/10.1021/jf00051a004.